Appl. Sci. Res. **21** August 1969

ON LAMINAR FLOW THROUGH A UNIFORMLY POROUS PIPE

R. M. TERRILL and P. W. THOMAS

Dept. of Applied Mathematics
The University of Liverpool,
Liverpool, U.K.

Abstract

Numerous investigations ([1] and [4–9]) have been made of laminar flow in a uniformly porous circular pipe with constant suction or injection applied at the wall. The object of this paper is to give a complete analysis of the numerical and theoretical solutions of this problem. It is shown that two solutions exist for all values of injection as well as the dual solutions for suction which had been noted by previous investigators. Analytical solutions are derived for large suction and injection; for large suction a viscous layer occurs at the wall while for large injection one solution has a viscous layer at the centre of the channel and the other has no viscous layer anywhere. Approximate analytic solutions are also given for small values of suction and injection.

Nomenclature

General

r	distance measured radially
z	distance measured along axis of pipe
u	velocity component in direction of z increasing
v	velocity component in direction of r increasing
p	pressure
ρ	density
ν	coefficient of kinematic viscosity
a	radius of pipe
V	velocity of suction at the wall
η	r^2/a^2
R	wall or suction Reynolds number, Va/ν
$f(\eta)$	similarity function defined in (6)
$u_0(\eta)$	eigensolution
$U(0)$	a velocity at $z = 0$
K	an arbitrary constant
B_K	Bernoulli numbers

Particular
Section 5

ε perturbation parameter, $-\frac{2}{R}$
β^2 a constant, $-K\varepsilon$
$x = \eta/\varepsilon$
$g(x) = f(\eta)/\varepsilon$

Section 6

ε perturbation parameter, $-\frac{R}{2}$
β^2 a constant, $-K\varepsilon$
$g(\eta) = \varepsilon f(\eta)$
$g_c(\eta) = g(\eta)$ near centre of pipe
η^* point where $g'(\eta) = 0$

Section 7

$\varepsilon = \frac{2}{R}$
$\beta^2 = K\varepsilon$
$t = (1 - \eta)/\varepsilon$
$w(t, \varepsilon) = [1 - f(t)]/\varepsilon$
α_0, α_1 constants
$g(\eta) = f(\eta) - \alpha_0\eta$
$\alpha = \alpha_0/\varepsilon$
γ_0 a constant
η^* point where $f''(\eta) = 0$

§ 1. Introduction

The effect of porous boundaries on the flow of fluids has been studied in detail in recent years since they are of interest in a wide range of problems, from paper making to the cooling of rocket and jet motors. For a general boundary shape and for a prescribed suction distribution on the boundary, it is necessary to solve a system of partial differential equations, but, in the case of channel and pipe flow, Berman [1] has shown that, for constant suction or injection at the walls, the problem may be reduced to solving a single ordinary nonlinear differential equation.

The solution of the problem of laminar flow in a uniformly porous channel has been discussed by various authors; a résumé of the numerical and theoretical work can be found in Terrill [2, 3]. The solutions of the appropriate differential equation are unique and appear to be stable and well behaved. In contrast, previous

numerical work on the problem of flow in a porous pipe, by Berman [4] and White [5], showed that the solutions exhibit a marked instability, with no solutions obtainable for some values of the wall suction, and dual solutions for all other values of the suction. Yuan and Finkelstein [6] obtained analytic solutions valid for large injection and for small suction and injection, by using a regular perturbation technique, but they found no indication of dual solutions. Berman [4], using a method of averages developed by Morduchow [7], had some success in predicting the duality for a limited range of small suction at the wall.

The numerical results of the present investigation show that dual solutions exist, not only for all values of the wall suction, but also for the whole range of wall injection. An attempt is made to explain this duality analytically, for various ranges of suction and injection.

The solution for large injection, obtained by [6], is surprising since it does not have a viscous layer at the centre, in contrast with the corresponding solution for parallel plates (see [3]). However, it appears from numerical results that the second solution obtained for the pipe has a viscous layer at the centre. Confirmation of this result is obtained analytically by the method of inner and outer expansions.

The solution for small suction and injection given by [6] agrees with the numerical results of this investigation but, as mentioned earlier, a second solution also exists. The second solution is found analytically by appealing to numerical results to determine the dominant terms in the differential equation. The resulting solution confirms the numerical results.

Examination of the numerical results for the large suction solutions shows that both solutions tend to the same limiting profile, which is of the boundary layer form. An analytic solution is obtained, by the method of inner and outer expansions, which agrees to first order with both solutions. It is found numerically and confirmed theoretically, that the two solutions differ by exponentially small terms, but the present authors are unable to obtain two separate analytic solutions valid throughout the pipe.

§ 2. The equations of motion

Consider steady, incompressible laminar flow through a pipe of

circular cross section with porous walls. Assuming that the flow is axisymmetric, we have that the equations of motion are

$$u\frac{\partial u}{\partial z}+v\frac{\partial u}{\partial r}=-\frac{1}{\rho}\frac{\partial p}{\partial z}+\frac{\nu}{r}\left[\frac{\partial}{\partial r}\left(r\frac{\partial u}{\partial r}\right)+\frac{\partial}{\partial z}\left(r\frac{\partial u}{\partial z}\right)\right], \tag{1}$$

$$u\frac{\partial v}{\partial z}+v\frac{\partial v}{\partial r}=-\frac{1}{\rho}\frac{\partial p}{\partial r}+\frac{\nu}{r}\left[\frac{\partial}{\partial r}\left(r\frac{\partial v}{\partial r}\right)+\frac{\partial}{\partial z}\left(r\frac{\partial v}{\partial z}\right)-\frac{v}{r}\right]. \tag{2}$$

The equation of continuity is

$$\frac{\partial}{\partial z}(ru)+\frac{\partial}{\partial r}(rv)=0. \tag{3}$$

At the wall the boundary conditions require the tangential velocity to be zero and the radial velocity to be the prescribed velocity of suction V. The boundary conditions on the axis are obtained by taking the flow to be symmetrical, so that

$$\begin{aligned} &u(z,a)=0, \quad v(z,a)=V, \\ &\left(\frac{\partial u}{\partial r}\right)_{r=0}=0, \quad v(z,0)=0. \end{aligned} \tag{4}$$

To obtain a solution it will be assumed that v is independent of z.

For simplification the dimensionless variable

$$\eta=r^2/a^2 \tag{5}$$

is introduced. The velocity component v will be taken in the non-dimensional form

$$v=\frac{Vf(\eta)}{\eta^{\frac{1}{2}}}, \tag{6}$$

where $f(\eta)$ is some function of η to be determined. Integration of (3) yields

$$u=-\frac{2Vf'(\eta)\,z}{a}+u_0(\eta) \tag{7}$$

where $u_0(\eta)$ is an arbitrary function of η. It has been assumed that v is independent of z and, therefore, differentiating (2) with respect to z gives

$$\frac{\partial^2 p}{\partial r\,\partial z}=0 \quad \text{or} \quad \frac{\partial^2 p}{\partial \eta\,\partial z}=0. \tag{8}$$

If u and v are substituted from (7) and (6) equation (2) yields

$$\frac{2V^2ff'}{\eta} - \frac{V^2f^2}{\eta^2} = -\frac{2}{\rho}\frac{\partial p}{\partial \eta} + \frac{4V\nu f''}{a}. \tag{9}$$

The pressure distribution is given by the integration of (9) with respect to η; hence

$$\frac{p}{\rho} = V^2\left[2R^{-1}f' - \frac{f^2}{2\eta}\right] + P(z), \tag{10}$$

where $P(z)$ is an arbitrary function of z, and where

$$R = \frac{Va}{\nu} \tag{11}$$

is the wall Reynolds number. If p is substituted from (10) into (1) it can be readily shown that $P(z)$ takes the form

$$P(z) = Az^2 + Bz + C, \tag{12}$$

where A, B, and C are constants. Substitution for u, v, and p from (7), (6), and (10) into (1) and equating the coefficients of z and z^0 yields

$$\eta f''' + f'' + \frac{R}{2}(f'^2 - ff'') = K \tag{13}$$

and

$$\eta u_0'' + u_0' + \frac{R}{2}(u_0f' - u_0'f) = d, \tag{14}$$

where the constants K and d are related to the constants A and B in (12) by

$$A = -\frac{4V^2K}{Ra^2}, \quad B = \frac{4Vd}{Ra}.$$

The boundary conditions (4) become

$$f'(1) = 0, \quad f(1) = 1, \quad f(0) = 0, \quad \lim_{\eta\to 0} \eta^{\frac{1}{2}}f''(\eta) = 0 \tag{15}$$

and

$$u_0(1) = 0, \quad \lim_{\eta\to 0} \eta^{\frac{1}{2}}u_0'(\eta) = 0. \tag{16}$$

Thus, the problem reduces to solving the differential equations (13) and (14) subject to the boundary conditions (15) and (16). A

particular solution of (14) is $u_0(\eta) \sim f'(\eta)$. Any further solutions of (14) can be regarded as eigensolutions.

In the region where the flow appears to be well behaved, it is of interest to know whether eigensolutions exist. Numerical results suggest that the solutions for large and small injection, denoted in Fig. 1 by Section I, are well behaved. Solutions for this range have been given by [6] and have been confirmed numerically. Although it is not intended to fully discuss the possibility of eigensolutions occurring for the complete range of wall suction and injection, it is a simple matter to consider eigensolutions for section I injection solutions. This possibility will now be discussed.

By a suitable choice of origin for z, the constant d in (14) may be taken to be zero. Then (14) may be written

$$\frac{\mathrm{d}}{\mathrm{d}\eta}(Fu_0') - Gu_0 = 0, \tag{17}$$

where

$$F = \eta \exp\left(-\int_0^\eta \frac{Rf}{2\eta}\mathrm{d}\eta\right) > 0 \quad \text{for} \quad \eta > 0$$

and

$$G = -\frac{Rf'F}{2}.$$

Numerical results and perturbation solutions for section I injection solutions show that $f'(\eta) \geqslant 0$ in the interval (0, 1). Thus, since $R \leqslant 0$ for this range, $G \geqslant 0$ in (0, 1). Then it follows from the Sturm-Liouville theory that the solutions of (14) are non-oscillatory. Hence there are no eigensolutions for section I injection solutions. However, it is possible that eigensolutions occur for other ranges. For the present these will be ignored, and only the particular case $u_0(\eta) \sim f'(\eta)$ will be taken. This is equivalent to taking (7) in the form

$$u = \left[U(0) - \frac{2Vz}{a}\right] f'(\eta).$$

The velocity profile $U(0)\, f'(\eta)$ may be regarded as the velocity distribution at $z = 0$. The numerical solution of (13) subject to boundary conditions (15) will be discussed in the following section and theoretical solutions will be obtained in sections 5, 6, and 7.

§ 3. Numerical method of solution

To solve (13) numerically subject to the boundary conditions (15) appears to require a double infinity of integrations for any prescribed Reynolds number, since the equation is a boundary value problem with two conditions at either end of the range. However, by making a suitable transformation and allowing R to be determined by the integration, the equation can be solved by only one integration.

Consider the transformation

$$f(\eta) = \lambda g(\xi)$$

$$\eta = \xi/b,$$

where λ and b are constants to be determined. Then substitution into (13) yields

$$\lambda b^2 \xi g''' + \lambda b^2 g'' + \frac{R}{2} \lambda^2 b^2 (g'^2 - gg'') = K, \tag{18}$$

where primes denote differentiation with respect to ξ. By choosing $\lambda R = 2$, we reduce (18) to

$$\xi g''' + g'' + g'^2 - gg'' = K_1 \tag{19}$$

where $K_1 = K/\lambda b^2$. From (15), the boundary conditions on (19) become

$$g(0) = g'(b) = 0 \qquad g(b) = \frac{1}{\lambda} = \frac{R}{2} \qquad \lim_{\xi \to 0} \xi^{\frac{1}{2}} g''(\xi) = 0. \tag{20}$$

The problem can now be solved by one integration using a step by step method. Arbitrary values are assigned to $g'(0)$ and $g''(0)$, and K_1 is then evaluated. The integration is then allowed to proceed until the required zero of $g'(\xi)$ is obtained. It is then possible to evaluate the interval b and the Reynolds number R, and, by making the inverse transformation, $f(\eta)$ and the constant K can be obtained.

Near $\xi = 0$, the step by step process of integration breaks down due to the term $\xi g'''$ in (19). Because of this difficulty a Taylor expansion was used in the neighbourhood of $\xi = 0$ and the Runge-Kutta procedure thereafter. As a check for accuracy both the step length and the take over point from the Taylor series to the Runge-Kutta procedure were varied.

§ 4. Discussion of numerical results

Numerical solutions were sought for all values of the wall Reynolds number $R(-\infty < R < \infty)$ and the results are most clearly seen by reference to Fig. 1. In this figure $f''(1)$, which is proportional to the skin friction at the wall, is plotted against R. It can be seen that dual solutions exist everywhere except in the range $2.3 < R < 9.1$, where no solutions were found. This range agrees with previous numerical work on the problem (notably with [4, 5]). In an attempt to show why no solutions existed in this range Weissberg [8] considered the inlet profile and, using Morduchow's [7] method of averages, concluded that in approximately this range of Reynolds number, fully developed flow could not be realized.

The results shown in Fig. 1 will now be considered in more detail. In order to facilitate discussion of the solutions and derivation of theoretical solutions, it will be convenient to subdivide Fig. 1 into five sections, as follows:

(1) Section I ($R = -\infty$ to $R = 2.3$) contains all the well behaved solutions for injection and the solutions for small suction up to the point where $f''(1)$ vanishes.

(2) Section II ($R = 2.3$ to $R = 0$) includes all the small suction solutions for which $f''(1) > 0$. These solutions have reverse flow near the wall of the tube.

(3) Section III ($R = -\infty$ to $R = 0$) covers the solutions for small and large injection Reynolds numbers, the velocity profiles being

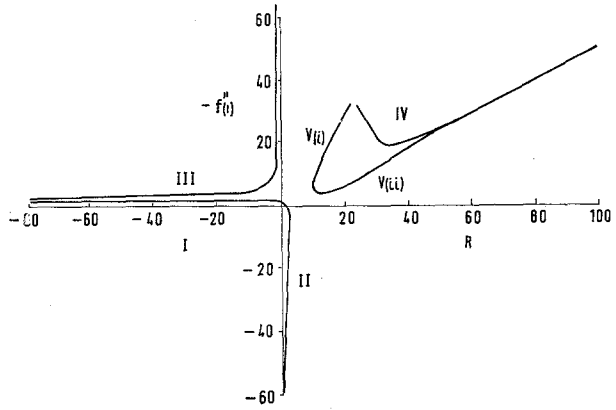

Fig. 1. Variation of $f''(1)$ with R for all values of suction and injection at the walls.

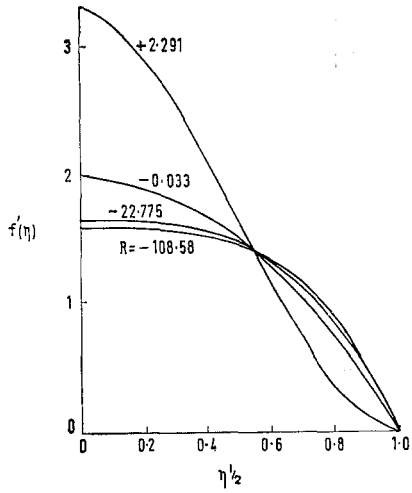

Fig. 2. Axial velocity $f'(\eta)$ against nondimensional radial distance $\eta^{\frac{1}{2}}$ for section I wall suction and injection.

characterized by a region of reverse flow at the centre of the pipe. (4) Section IV ($R = 21.2$ to $R = \infty$) contains all the solutions for suction Reynolds numbers greater than 21.2 on the upper branch of Fig. 1. These velocity profiles have two turning points and a minimum between the axis and the pipe wall.

(5) Section V covers all the remaining solutions, the velocity profiles being characterized by a single point of inflexion. Although dual solutions are included in section V for the range $9.1 < R < 21.2$, this choice is justified since the deformation of the velocity profile throughout this section is continuous. Section V is divided into two regions, V(i), which covers the solutions for the range $9.1 < R < 21.2$ on the upper branch, and V(ii) which includes all solutions in the range $9.1 < R < \infty$ on the lower branch.

Fig. 2 shows velocity profiles for section I. For all values of the injection Reynolds number and for very small suction Reynolds numbers the profiles are well behaved. Very little change occurs in the profiles, with the nondimensional centre line velocity changing from a little less than 1.6 for large injection to about 2.0 for zero suction and to approximately 3.3 when the skin friction at the wall vanishes (i.e. at $R = 2.3$). These results agree with those obtained by [5, 4, 9] and with the regular perturbation solutions for large injection and for small suction and injection given by [6].

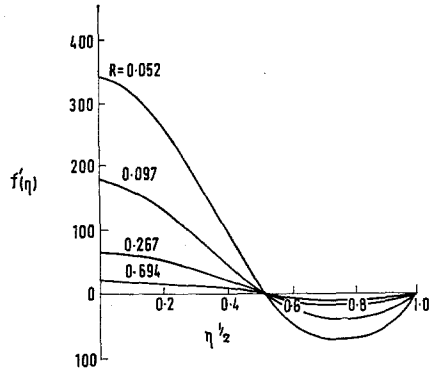

Fig. 3. Axial velocity profiles for section II wall suction.

Velocity profiles for section II are given in Fig. 3. These are characterized by a rapid increase in the centre line velocity as R decreases from the value 2.3, and the development of reverse flow near the wall of the pipe. The profiles represent a continuous deformation from those of section I, the limiting profiles as $f''(1) \to 0^+$ and 0^- being identical. As $R \to 0$ both the centre line velocity and the skin friction at the wall tend to infinity. White [5] suggested the existence of section II solutions, and Berman [4] was able to obtain these solutions in the range $2.0 < R < 2.3$ and verify the results using Morduchow's method of averages.

Section III velocity profiles are given in Fig. 4. These solutions, which have not been obtained in previous work, are characterized for both large and small injection by a region of reverse flow at the centre of the pipe. For large injection this region becomes increasingly small, and the limiting profile is the same as that for large injection solutions in section I, but with a point discontinuity due to a viscous layer at the centre of the pipe. At the other end of the range, as the injection Reynolds number decreases to zero, both the nondimensional centre line velocity and the skin friction at the wall tend to minus infinity. Reference to Fig. 5 shows that the velocity profile obtained for small injection (section III) is, to first order, the reflection in the η-axis of that obtained for small suction (section II) and, in fact, when $R = 0^{\pm}$ the limiting profiles are exact images of one another. This conclusion will be clarified in section 6.

Typical profiles for section IV solutions are given in Fig. 6. It can

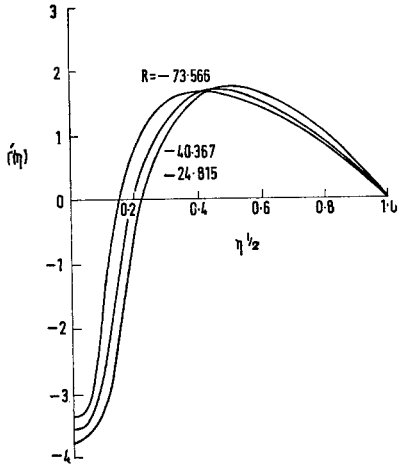

Fig. 4(1).

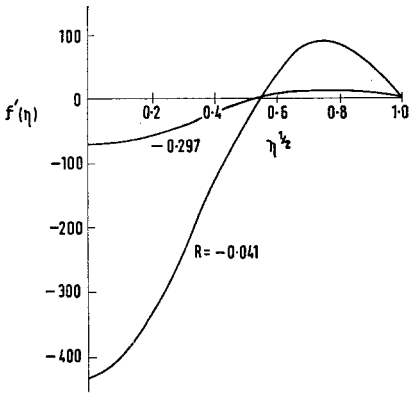

Fig. 4(2).

Fig. 4(1). Axial velocity profiles for section III wall injection, for large Reynolds numbers.

Fig. 4(2). Axial velocity profiles for section III wall injection, for small Reynolds numbers.

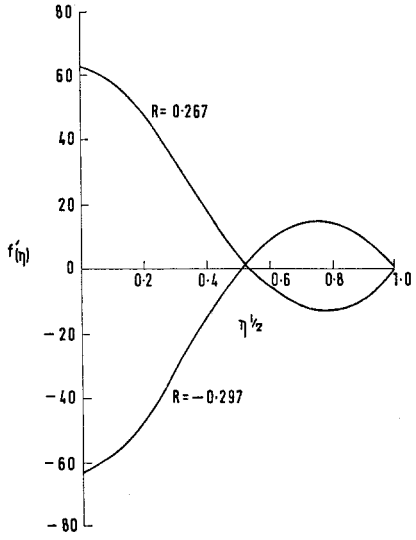

Fig. 5.

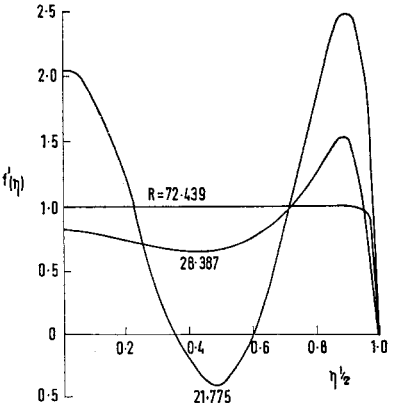

Fig. 6.

Fig. 5. Comparison of the velocity profiles for small suction and small injection (sections II and III).

Fig. 6. Axial velocity profiles for section IV, wall suction.

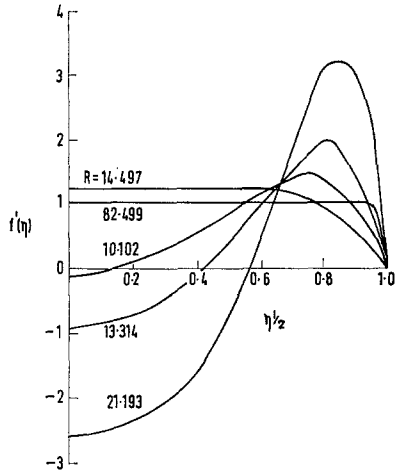

Fig. 7. Axial velocity profiles for section V, wall suction.

be seen that they are characterized by two points of inflexion and a minimum between the axis and the wall of the pipe. In the range $21.2 < R < 23$ a region of reverse flow occurs in the neighbourhood of this minimum velocity. As $R \to \infty$ the velocity profiles take on the familiar boundary layer shape with a maximum velocity very close to the mean velocity.

Fig. 7 gives velocity profiles for section V solutions. The profiles $R = 10.102$, 13.314, 21.193 represent solutions on V(i) whereas the profiles $R = 14.497$, $R = 82.499$ represent solutions on V(ii). For large suction the profiles also assume the boundary layer form, the limiting profiles for sections IV and V being identical. Berman [4] who first noted the existence of section IV solutions as an apparently independent set of profiles, did not show the asymptotic nature of the two solutions for large R. The behaviour of the two solutions for large suction will be discussed in section 7, where it will be shown that an asymptotic expansion is equally valid for both solutions and that the difference between the solutions decreases exponentially as $R \to \infty$. As R decreases from infinity, the centre line velocity and the skin friction at the wall decrease until, when $R = 10.1$, reverse flow develops at the centre of the pipe. This becomes more pronounced in section V(i) solutions as $R \to 21.2$.

The characteristics of the velocity profiles of sections IV and V(i) are different and, at first sight, would appear only to be linked

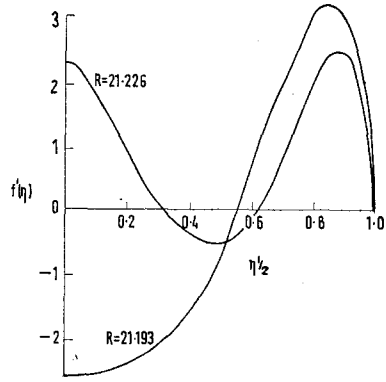

Fig. 8. Axial velocity profiles for Reynolds numbers $R \approx 21.2$.

through their behaviour for large suction. However, consideration of Fig. 8, which shows velocity profiles for R just greater than and just less than 21.2, suggests that as $R \to 21.2$ from above and below (section IV and V(i), respectively) the limiting profiles are identical but for a point singularity at $\eta = 0$. This is more clearly seen by reference to Fig. 9, which shows a plot of $f''(0)$ against R. As $R \to 21.2^+$ the function $f''(0) \to \infty$ while $f''(0)$ remains finite and is well behaved for $R \to 21.2^-$. This singularity explains why White [5], using a series method and then solving numerically by a computer, was unable to obtain section IV solutions, since obviously a series method breaks down at this point.

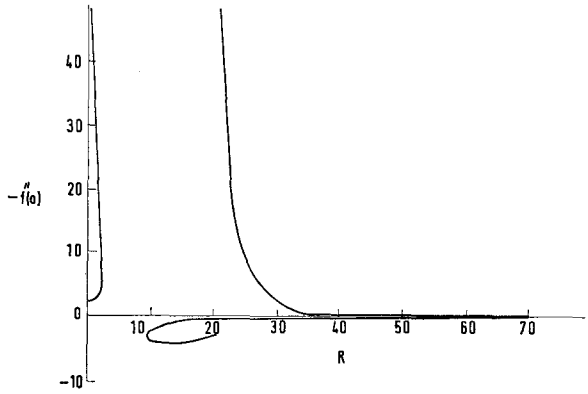

Fig. 9. Variation of $f''(0)$ with R for a range of values of wall suction.

The solutions for the complete range of Reynolds numbers ($-\infty < R < \infty$) show a marked degree of symmetry. Section I and III solutions are identical for large injection but with a point discontinuity at $\eta = 0$, section II and III solutions are, to first order, reflections of one another for small Reynolds numbers, section IV and V(ii) solutions are asymptotically equal, and section IV and V(i) solutions for $R = 21.2$ differ by a singularity at $\eta = 0$.

§ 5. Solution for large injection Reynolds numbers

The solution of (13) subject to the boundary conditions (15), for large injection Reynolds numbers, has been obtained by [6] using a regular perturbation technique. This solution agrees with the numerical solutions obtained for section I large injection, but gives no indication of the possibility of a second solution. However, numerical results show that, for section III large injection, a solution is obtained where the axial velocity changes rapidly near the centre of the pipe but which behaves like the section I solution away from the axis. In this section this second solution will be obtained using the method of inner and outer expansions.

Equation (13) may be written

$$\varepsilon(\eta f''' + f'') - f'^2 + ff'' = -\beta^2, \tag{21}$$

where $\varepsilon = -2/R > 0$, and $K\varepsilon = -\beta^2$. Assume a solution of the form

$$f(\eta) = \sum_{n=0}^{\infty} f_n(\eta)\, \varepsilon^n, \quad \beta = \sum_{n=0}^{\infty} \beta_n \varepsilon^n.$$

Then equating coefficients of ε^p ($p = 0, 1, 2, \ldots$) yields the equations

$$f_0'^2 - f_0 f_0'' = \beta_0^2, \tag{22}$$

$$\eta f_0''' + f_0'' - 2f_0' f_1' + f_0 f_1'' + f_1 f_0'' = -2\beta_0\beta_1, \tag{23}$$

$$\cdots\cdots\cdots\cdots\cdots\cdots\cdots\cdots\cdots\cdots$$

Equations (22), (23), ... are solved subject to the boundary conditions at the wall, namely,

$$f_0(1) = 1, \quad f_n(1) = 0 \quad \text{for} \quad n \neq 0, \quad f_n'(1) = 0. \tag{24}$$

In formulating this solution the highest derivative of (21) is neglected. Should there be an inner region, where the highest derivative is significant, then this solution will break down and it will be valid as an outer solution only.

The solution of (22) subject to the boundary conditions (24) is

$$f_0(\eta) = \cos(\beta_0(\eta - 1)). \tag{25}$$

This solution can be made to satisfy all boundary conditions provided $\beta_0 = \pi/2$ and is then valid throughout $0 \leqslant \eta \leqslant 1$.

It is now possible to obtain a second perturbation solution which satisfies all boundary conditions by solving (23). The series solution so obtained will be shown to correspond to the section I numerical solutions for large injection.

However, it is known from numerical results that for large injection a second solution exists which is not well behaved at $\eta = 0$. To obtain an analytical expression for this solution (22) and (23) will be regarded as the equations for the outer solution and the outer solution will be matched with an inner solution valid near the centre of the pipe.

When $\beta_0 = \pi/2$, equation (25) yields

$$f_0(\eta) = \sin\frac{\pi\eta}{2}. \tag{26}$$

Then (23) becomes

$$\sin\frac{\pi\eta}{2} f_1'' - \pi\cos\frac{\pi\eta}{2} f_1' - \frac{\pi^2}{4}\sin\frac{\pi\eta}{2} f_1 =$$

$$= -\pi\beta_1 + \frac{\pi^2}{4}\sin\frac{\pi\eta}{2} + \frac{\pi^3\eta}{8}\cos\frac{\pi\eta}{2}. \tag{27}$$

The solution of (27), subject to boundary conditions (24), is

$$f_1(\eta) = \left\{\frac{\pi}{2}\left(1 - \frac{4\beta_1}{\pi}\right) - \frac{\pi^3}{16}\int_1^\eta \frac{\xi^2\,\mathrm{d}\xi}{\sin\frac{\pi\xi}{2}}\right\}\cos\frac{\pi\eta}{2} +$$

$$+\left\{\frac{\pi}{2}\left(\frac{3}{2} - \frac{4\beta_1}{\pi}\right) - \frac{\pi^3}{16}\int_1^\eta \frac{\xi\,\mathrm{d}\xi}{\sin\frac{\pi\xi}{2}}\right\}\left\{\frac{2}{\pi}\sin\frac{\pi\eta}{2} - \eta\cos\frac{\pi\eta}{2}\right\} -$$

$$-\left(\frac{3}{2} - \frac{4\beta_1}{\pi}\sin\frac{\pi\eta}{2}\right). \tag{28}$$

To find a solution valid throughout the range $0 \leqslant \eta \leqslant 1$ the initial

conditions must be satisfied. The condition

$$\lim_{\eta \to 0} \eta^{\frac{1}{2}} f''(\eta) = 0$$

is automatically satisfied by $f_1(\eta)$, and if the condition $f_1(0) = 0$ is imposed, a value

$$\beta_1 = 0.422$$

is obtained. Then (26) and (28) together give a second perturbation solution $f_0(\eta) + \varepsilon f_1(\eta)$ which satisfies all boundary conditions. This is the regular perturbation solution obtained by [6], and corresponds to the solutions in section I for large injection (Fig. 1). A comparison of the results obtained by perturbation and numerically is given in Table I, where $f''(1)$ is given for a range of Reynolds numbers.

TABLE I

$-R$	numerical $-f''(1)$	calculated $-f''(1)$	corrected $-f''(1)$
24.19906	2.457	2.483	2.449
33.72519	2.4637	2.4783	2.4610
44.66713	2.4667	2.4756	2.4658
55.60832	2.4680	2.4740	2.4677
80.36234	2.46905	2.47196	2.46893
91.64563	2.469085	2.471402	2.469069
102.9344	2.469112	2.470963	2.469112
151.3834	2.468955	2.469823	2.468967
241.9763	2.468579	2.468916	2.468576

The quantity $f''(1)$ against R for large injection (section I solutions).

The second order perturbation solution yields results which differ from the numerical results to some extent. To test the accuracy of the series further, a third order correction term was calculated. The corrected series was found to be

$$f''(1) = -\frac{\pi^2}{4} - 0.1833\varepsilon + 4.9031\varepsilon^2,$$

and it can be seen from Table I that the values for the corrected series and the numerical solution are extremely close.

The solution obtained must break down near the centre of the pipe if a viscous layer exists. No guide as to the range of discon-

tinuity can be obtained from the outer expansion since it has been shown that a regular second order perturbation solution exists in addition to the possible viscous layer solution. Also, unlike the solution for laminar flow between porous parallel plates [3], an analysis of (21) gives no indication of possible discontinuities in $f(\eta)$ or its derivatives. The only guide, therefore, to obtaining the inner expansion is by appeal to numerical results. The outer expansion was taken to be $f(\eta) = f_0(\eta) + \varepsilon f_1(\eta) + \ldots$, where $f_1(\eta)$, given by (28), has an arbitrary constant β_1 to be determined by matching with the proposed inner expansion.

To obtain the inner solution a suitable stretching transformation must be used.

Consider a transformation of the form $\eta = \varepsilon^r x$, $f(\eta) = \varepsilon^p g(x)$. Substitution into (21) yields

$$\varepsilon(x\varepsilon^p g''' + \varepsilon^p g'') - \varepsilon^{2p} g'^2 + \varepsilon^{2p} g g'' = -\beta^2 \varepsilon^{2r}. \tag{29}$$

If the inertial terms are not to dominate the viscous terms then $p \geqslant 1$. If $p > 1$ then a first approximation to (29) gives

$$\begin{aligned} x g''' + g'' &= 0 \qquad & 2r > p + 1 \\ x g''' + g'' &= -\beta^2 \qquad & 2r = p + 1. \end{aligned}$$

These equations imply that either $g''(\eta) = 0$ or $g'''(\eta) = 0$. Matching with the outer solution shows that neither can be the solution and so $p = 1$. Then (29) yields

$$x g''' + g'' - g'^2 + g g'' = -\beta^2 \varepsilon^{2(r-1)}, \qquad r \geqslant 1. \tag{30}$$

Without loss of generality it may be assumed that $r = 1$. Then the equation to be solved for the inner solution is

$$x g''' + g'' - g'^2 + g g'' = -\beta^2. \tag{31}$$

Equation (31) is nonlinear and so it is virtually impossible to obtain a general inner solution containing arbitrary constants. Instead, an inner solution will be obtained that fits (31) identically, satisfies the boundary conditions at the centre of the pipe, and tends asymptotically to the outer solution.

A perturbation of (31) of the form $g(x) = \sum_{n=0}^{\infty} g_n(x)\, \varepsilon^n$ yields

$$x g_0''' + g_0'' - g_0'^2 + g_0 g_0'' = -\beta_0^2, \tag{32}$$

$$xg_1''' + g_1'' - 2g_0'g_1' + g_0g_1'' + g_1g_0'' = -2\beta_0\beta_1, \qquad (33)$$

.....

where $\beta_0 = \pi/2$.

Equation (32) can be solved by a power series solution of the form $g_0(x) = \sum_0^\infty a_n x^n$ and, applying the boundary conditions at the centre of the pipe, we find as solution

$$g_0(x) = a_1 x + \left(a_1^2 - \left(\frac{\pi}{2}\right)^2\right)\frac{x^2}{2} + a_1\left(a_1^2 - \left(\frac{\pi}{2}\right)^2\right)\frac{x^3}{12} + \\ + \left(a_1^2 - \left(\frac{\pi}{2}\right)^2\right)^2 \frac{x^4}{72} + \dots . \qquad (34)$$

The value $a_1 = \pi/2$ yields $g_0(x) = \pi x/2$, which is an approximation for small η to the first term of the outer solution. However, it is possible to obtain a second solution when $a_1 = -\pi$. Equation (34) then takes the form

$$g_0(x) = -\pi x + \frac{3\pi^2 x^2}{8} - \frac{3\pi^3 x^3}{48} + \frac{9\pi^4 x^4}{1152} + \dots, \qquad (35)$$

a result representing the first few terms of

$$g_0(x) = \frac{\pi x}{2} - 3 + 3\exp\left(-\frac{\pi x}{2}\right). \qquad (36)$$

This solution is an approximation to (35), but substitution into (31) shows that the solution for $g_0(x)$ satisfies the equation identically. Now as $x \to \infty$, $g_0(x) \to \pi x/2$ and so $f_0(\eta) \to \pi\eta/2$. Thus, the solution given by (36) tends asymptotically to the outer solution at the edge of the viscous layer.

From equations (26) and (28) the first two terms of the outer expansion are

$$f(\eta) = \sin\frac{\pi\eta}{2} + \varepsilon\left\{\frac{\pi}{2}\left(1 - \frac{4\beta_1}{\pi}\right) - \frac{\pi^3}{16}\left(\int_1^\eta \frac{\xi^2\,d\xi}{\sin\frac{\pi\xi}{2}}\right)\cos\frac{\pi\eta}{2} + \right.$$

$$+ \left[\frac{\pi}{2}\left(\frac{3}{2} - \frac{4\beta_1}{\pi}\right) - \frac{\pi^3}{16}\int_1^\eta \frac{\xi\,d\xi}{\sin\frac{\pi\xi}{2}}\right]\left[\frac{2}{\pi}\sin\frac{\pi\eta}{2} - \eta\cos\frac{\pi\eta}{2}\right] -$$

$$\left. - \left[\frac{3}{2} - \frac{4\beta_1}{\pi}\sin\frac{\pi\eta}{2}\right]\right\}, \qquad (37)$$

where

$$\int \xi \operatorname{cosec} \frac{\pi\xi}{2} \, d\xi = \frac{2\xi}{\pi} + \sum_{K=1}^{\infty} \frac{2(2^{2K-1} - 1)|B_{2K}|}{(2K+1)!} \left(\frac{\pi}{2}\right)^{2K-1} \xi^{2K+1}$$

$$\int \xi^2 \operatorname{cosec} \frac{\pi\xi}{2} \, d\xi = \frac{\xi^2}{\pi} + \sum_{K=1}^{\infty} \frac{2(2^{2K-1} - 1)|B_{2K}|}{(2K+1)!} \times \left(\frac{\pi}{2}\right)^{2K-1} \xi^{2K+2}$$

and B_{2K} $(K = 1, 2, \ldots)$ are the Bernoulli numbers. The first two terms of the outer expansion in inner variables are

$$f(x) = \frac{\pi\varepsilon x}{2} + \varepsilon \left\{ \frac{\pi}{2} \left(1 - \frac{4\beta_1}{\pi}\right) - \pi - \right.$$

$$\left. - \frac{3}{2} + \frac{\pi^3}{16} \left[\frac{1}{\pi} + \sum_{K=1}^{\infty} 2(2^{2K-1} - 1)|B_{2K}| \times \right.\right.$$

$$\left.\left. \times \left(\frac{\pi}{2}\right)^{2K-1} (2K+1) \right] \right\} + O(\varepsilon^2). \tag{38}$$

When matched with the inner expansion this yields

$$\beta_1 = 1.9224.$$

An attempt was made to solve (33) to obtain the second term of the inner expansion, but beyond finding one complementary function this proved to be impossible.

Numerical and theoretical values for $f''(1)$ and $f''(0)$ are given in Table II. The values of $f''(1)$, proportional to the skin friction at the wall, enable one to compare the outer solution with the numerical

TABLE II

	numerical		asymptotic		
R	$f''(0)$	$f''(1)$	$f''(0)$	$f''(1)$	$[f''(0)]$
−24.815	132.2	−3.259	91.8	−3.242	40.4
−40.367	188.2	−2.950	149.9	−2.943	38.8
−55.817	244.6	−2.815	206.5	−2.811	38.1
−66.034	282.2	−2.761	244.3	−2.758	37.9
−73.566	308.9	−2.731	272.2	−2.729	36.7

Numerical and asymptotic values of $f''(0)$ and $f''(1)$ for large injection Reynolds numbers (section III solutions), $[f''(0)]$ is the difference between the numerical and the analytical values of $f''(0)$.

results whereas the values of $f''(0)$ can be used to confirm the inner solution.

The outer solution, given by (37), should be accurate to the second order; that is, the neglected terms are of order ε^2. This is confirmed by the numerical solutions. There is considerable difference between the numerical and theoretical values for $f''(0)$. However, the theoretical solution given by (36) is accurate only to order $1/\varepsilon$. Thus, it is expected that the difference between the theoretical and numerical values for $f''(0)$ will be a constant and this is confirmed by the results in Table II.

§ 6. Solution for small Reynolds numbers

A solution for small R has been obtained in [6] by a regular perturbation of (13) of the form $f(\eta) = \sum_0^\infty f_r(\eta)\, \varepsilon^r$. When $\varepsilon = 0$ this gives the solution for impermeable flow, the profiles taking the familiar parabolic form. This solution gives accurate results in the range $-2 < R < 2$, but does not yield results in the region where the skin friction vanishes. Another solution by [4], based upon the method of averages given in [7], has some success in predicting the solutions beyond the point of vanishing skin friction. White [5], using a power series expansion, finds solutions up to the point where $f''(1)$ becomes zero. Beyond this point a power series expansion fails because the function f and its derivatives become increasingly large and tend to infinity as R tends to zero.

The purpose of this section is to obtain an approximate solution of (13) valid for small suction and for small injection Reynolds numbers in the regions II and III where reverse flow exists. Numerical results indicate that in regions II and III, when R is small, the functions $f^{(n)}(\eta)$ $(n = 0, 1, 2, \ldots)$ are of order $1/R$ and so a linear stretch of variable of the form $g(\eta) = \varepsilon f(\eta)$ is suggested, where $\varepsilon = -R/2$. Substitution into (13) yields

$$\eta g''' + g'' - g'^2 + gg'' = -\beta^2, \tag{39}$$

where $\beta^2 = -K\varepsilon$ is a constant to be determined, and the boundary conditions (15) become

$$g(0) = g'(1) = 0, \quad g(1) = \varepsilon, \quad \lim_{\eta \to 0} \eta^{\frac{1}{2}} g''(\eta) = 0. \tag{40}$$

The solution of (39), subject to the boundary conditions (40), will be to first order independent of ε. Hence, to first order the con-

dition on $g(\eta)$ at the wall may be taken as $g(1) = 0$, and, since $f^{(n)}(\eta) = \varepsilon^{-1}g^{(n)}(\eta)$ the solution for small injection will be everywhere the image of the solution for small suction.

If a power series of the form

$$g(\eta) = \sum_{n=0}^{\infty} a_n \eta^n$$

is substituted into (39), the solution, denoted by $g_c(\eta)$, satisfying the boundary conditions at $\eta = 0$ is found to be

$$g_c(\eta) = a_1\eta + \frac{(a_1^2 - \beta^2)}{2}\eta^2 + a_1\frac{(a_1^2 - \beta^2)}{12}\eta^3 + \\ + \frac{(a_1^2 - \beta^2)^2}{72}\eta^4 + \dots . \qquad (41)$$

A similar expansion was obtained for the inner solution for large injection and, as in that case, we will choose

$$a_1 = -2\beta,$$

so that $g_c(\eta)$ reduces to

$$g_c(\eta) = \beta\eta + 3\,e^{-\beta\eta} - 3. \qquad (42)$$

Although the solution (42) does not satisfy the boundary conditions at the wall, it gives an excellent approximation to numerical results between $\eta = 0$ and the point where $g_c'(\eta) = 0$. Equation (42) will be taken to be the solution near $\eta = 0$, and will be matched with a solution valid near $\eta = 1$.

The solution near $\eta = 1$. To first order, the boundary conditions to be satisfied by (39) at the wall are $g(1) = g'(1) = 0$. For small suction Reynolds numbers the viscous terms are small compared with the inertial terms in the neighbourhood of the wall $\eta = 1$. Thus, near $\eta = 1$ equation (39) reduces to

$$\eta g''' + g'' = -\beta^2. \qquad (43)$$

The solution of (44), subject to $g(1) = g'(1) = 0$, is

$$g(\eta) = \frac{\beta^2}{2}(\eta + \eta\ln\eta - \eta^2) + \alpha(1 + \eta\ln\eta - \eta), \qquad (44)$$

where α is an arbitrary constant. This solution, denoted by $g_0(\eta)$,

will be assumed to be valid between $\eta = 1$ and the point $\eta = \eta^*$ where $g_c'(\eta^*) = 0$.

From (42), $g_c'(\eta^*) = 0$ when

$$\eta^* = \beta^{-1} \ln 3. \tag{45}$$

Then $g_c(\eta^*) = \ln 3 - 2$, and the constants α and β are found by comparison of $g(\eta)$ and $g'(\eta)$ at $\eta = \eta^*$. Then

$$\ln 3 - 2 = \frac{\beta^2}{2}(\eta^* + \eta^* \ln \eta^* - \eta^{*2}) + \alpha(1 + \eta^* \ln \eta^* - \eta^*), \tag{46}$$

and

$$0 = \frac{\beta^2}{2}[2 + \ln \eta^* - 2\eta^*] + \alpha \ln \eta^*. \tag{47}$$

The solution of (45), (46), and (47) gives

$$\alpha = 0.971, \quad \beta = 4.025, \quad \eta^* = 0.273. \tag{48}$$

The solutions (42) and (44), where the constants are given by (48), give good agreement with numerical results for the whole range of η.

When the solution (44) was obtained it was assumed that the inertial terms could be neglected. While this assumption is valid near $\eta = 1$, the solution is required to be valid as far as $\eta = 0.273$. It is therefore necessary to consider the effect of the inertial terms on (44).

The series solution of (39) near $\eta = 1$ can be expressed as a power series in z, where $z = 1 - \eta$, in the form

$$g(z) = a_2 z^2 + a_3 z^3 + \frac{a_3}{2} z^4 + \left(\tfrac{3}{10} a_3 - \frac{a_2^2}{30}\right) z^5 +$$
$$+ \left(\tfrac{1}{5} a_3 - \frac{a_2^2}{45} - \frac{a_2 a_3}{30}\right) z^6 + \left(\tfrac{1}{7} a_3 - \frac{a_2^2}{63} - \frac{a_2 a_3}{35} - \frac{a_3^2}{70}\right) z^7 +$$
$$+ \left(\frac{3a_3}{28} - \frac{a_2^2}{84} - \frac{a_2^3}{5040} - \frac{11 a_2 a_3}{560} - \frac{11 a_3^2}{560}\right) z^8 + O(z^9), \tag{49}$$

where a_2 and a_3 are constants to be determined.

The solution $g_0(\eta)$ previously assumed can be expressed as a power series in z in the form

$$g_0(z) = \left(\frac{\beta^2}{2} + \alpha\right)\left(\frac{z^2}{2} + \frac{z^3}{6} + \frac{z^4}{12} + \frac{z^5}{20} + \frac{z^6}{30} + \cdots\right) - \frac{\beta^2 z^2}{2}. \tag{50}$$

Equations (49) and (50) together show that

$$a_2 = \frac{1}{2}\left(\alpha - \frac{\beta^2}{2}\right) \quad \text{and} \quad a_3 = \frac{1}{6}\left(\frac{\beta^2}{2} + \alpha\right)$$

and the correction to (50) is

$$g_1(z) = -\frac{a_2^2}{30} z^5 - \left(\frac{a_2^2}{45} + \frac{a_2 a_3}{30}\right) z^6 - \left(\frac{a_2^2}{63} + \frac{a_2 a_3}{35} + \frac{a_3^2}{70}\right) z^7 - \\ - \left(\frac{a_2^2}{84} + \frac{a_2^3}{5040} + \frac{11 a_2 a_3}{560} + \frac{11 a_3^2}{560}\right) z^8 + O(z^9). \qquad (51)$$

The solution $g(z) = g_0(z) + g_1(z)$ was matched with the solution $g_c(\eta)$ at the point $\eta = \eta^*$, and the modified values of α, β, and η^*, together with the correction terms, were obtained by an iterative process. The corrected solution gives

$$\alpha = 1.577, \quad \beta = 4.196, \quad \eta^* = 0.262, \qquad (52)$$

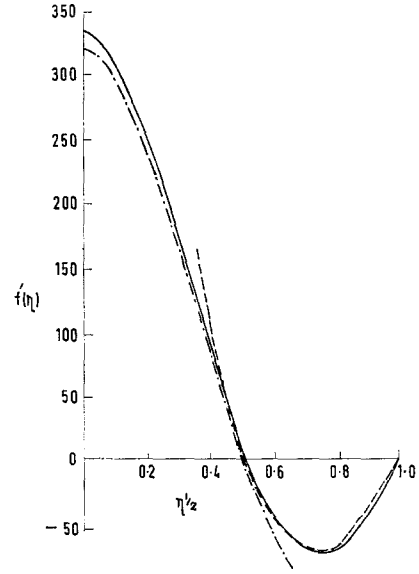

Fig. 10. Velocity profiles for $R = 0.052$ (section II):
numerical solution ————
analytic solution near $\eta = 0$ —·—·—·—
analytic solution near $\eta = 1$ — — — —.

TABLE III

	numerical		analytical	
R	$f''(0)$	$f''(1)$	$f''(0)$	$f''(1)$
−0.932	162	−22	113	−15
−0.592	231	−33	179	−24
−0.297	418	−61	356	−49
−0.041	2773	−416	2577	−353
0.052	−2105	319	−2032	278
0.141	−755	115	−749	103
0.267	−382	59	−396	54
0.346	−286	44	−305	42
0.422	−227	35	−250	34
0.564	−160	25	−187	26

Numerical and analytical values of $f''(0)$ and $f''(1)$ for small suction and injection Reynolds numbers (sections II and III).

and

$$g_c(\eta) = 4.196\eta + 3\exp[-4.196\eta] - 3, \tag{53}$$

$$g_0(\eta) + g_1(\eta) = 8.81(\eta + \eta\ln\eta - \eta^2) + 1.577(1 + \eta\ln\eta - \eta) - \\ - 0.435(1-\eta)^5 - 0.082(1-\eta)^6 - 0.071(1-\eta)^7 - \\ - 0.082(1-\eta)^8 + O[(1-\eta)^9]. \tag{54}$$

This solution shows that the effect of the inertial terms is not very significant even at $\eta = \eta^*$. Fig. 10 shows a plot of $g'(\eta)$ against η for the numerical and theoretical results, and it can be seen that for small Reynolds numbers agreement is extremely close. Table III gives numerical and theoretical values of $f''(1)$ and $f''(0)$ for small suction and injection Reynold numbers and shows that, within the limits of accuracy of the solution near the wall, agreement between the values is reasonably good. The difference between the numerical and the analytical values of $f''(0)$ is explained by an error of 3% in the evaluation of β.

§ 7. Solution for large suction Reynolds numbers

In this section a solution of (13), subject to the boundary conditions (15), is obtained for large suction by using the method of inner and outer expansions. Equation (13) may be written

$$\varepsilon(\eta f''' + f'') + f'^2 - ff'' = \beta^2, \tag{55}$$

where $\varepsilon = 2/R$ and $\beta^2 = K\varepsilon$. When there is large suction at the

wall it is, in general, expected that there will be a boundary layer at the wall; this is confirmed numerically for this problem (see Figs. 6 and 7), so that a perturbation solution of (55) valid outside the boundary layer would break down inside the layer as the viscous terms become dominant. For this reason an inner solution is sought which satisfies the conditions at the wall, and then is matched to the outer perturbation solution to determine the arbitrary constants.

7.1. *Outer expansion.* An expansion of the form $f(\eta) = \sum_0^\infty f_n(\eta)\,\varepsilon^n$, $\beta = \sum_0^\infty \beta_n \varepsilon^n$ is assumed. Then substitution into (55) and equating coefficients of ε^n yields

$$f_0'^2 - f_0 f_0'' = \beta_0^2, \tag{56}$$

$$\eta f_0''' + f_0'' + 2f_0' f_1' - f_0 f_1'' - f_1 f_0'' = 2\beta_0\beta_1, \tag{57}$$

$$\cdots\cdots\cdots\cdots\cdots\cdots\cdots\cdots\cdots\cdots\cdot$$

The boundary conditions (15) become, at the centre of the pipe,

$$f_n(0) = 0, \quad \lim_{\eta\to 0} \eta^{\frac{1}{2}} f_n''(\eta) = 0. \tag{58}$$

To obtain the outer expansion we must solve (56), (57), ... subject to the boundary conditions (58). Since the flow for large suction gives rise to boundary layers at the walls it seems physically reasonable that the outer solution should be of the form $f(\eta) \sim \eta$. However, since the flow appears to be unstable throughout much of the range of wall suction, it appears more satisfactory to argue from the numerical solutions. These also suggest a solution of the form

$$f_0(\eta) = \beta_0 \eta. \tag{59}$$

The solution of (57) and further perturbations produce polynomials in η^r. However, it will be shown that the inner solution expressed in outer variables only involves terms linear in η and exponentially small terms, so it is clear that the solutions of successive equations relating to the outer expansion are $f_r(\eta) = \beta_r \eta$. Hence

$$f(\eta) = \sum_{n=0}^{\infty} \beta_n \varepsilon^n \eta. \tag{60}$$

This form of the outer expansion agrees with numerical results, which shows that $f''(\eta)$ and higher derivatives are exponentially small outside the boundary layer. The outer expansion will be slightly modified later in this section to consider the leading exponentially small term.

7.2. *Inner expansion.* The outer expansion (60) breaks down near the wall of the pipe since it cannot satisfy the condition of no slip at the wall. To obtain a solution valid within the boundary layer a suitable stretch of variable must be employed to make the viscous and inertial terms of (55) of the same order near $\eta = 1$. It is easy to show that the appropriate stretching transformation is $1 - \eta = \varepsilon t$. Substitution into (55) gives

$$-(1 - \varepsilon t) f''' + \varepsilon f'' + f'^2 - ff'' = \beta^2 \varepsilon^2, \tag{61}$$

where primes denote differentiation with respect to t. Since the inner solution must tend asymptotically to the outer solution and satisfy the condition at the wall, $f(0) = 1$, the inner solution will be taken to be

$$f(t) = 1 - \varepsilon w(t, \varepsilon), \tag{62}$$

where

$$w(t, \varepsilon) = \sum_{n=0}^{\infty} w_n(t)\, \varepsilon^n. \tag{63}$$

Substitution into (61) and equating coefficients of ε^r yields

$$w_0''' + w_0'' = 0, \tag{64}$$

$$w_1''' - t w_0''' - w_0'' + w_0'^2 + w_1'' - w_0 w_0'' = \beta_0^2, \tag{65}$$

$$\cdots\cdots\cdots\cdots\cdots\cdots\cdots\cdots\cdots\cdots\cdots\cdots .$$

The boundary conditions at the wall become

$$w_n(0) = 0, \quad w_n'(0) = 0. \tag{66}$$

The solution of (64), subject to the boundary conditions (66), is

$$w_0 = A_0(t - 1 + e^{-t}), \tag{67}$$

where A_0 is an arbitrary constant. For simplicity the solution for each iteration will be matched to the outer solution to obtain the arbitrary constants. Then (62), (63), and (67) give the first two terms of the inner expansion

$$f(t) = 1 - \varepsilon A_0(t - 1 + e^{-t}). \tag{68}$$

Equation (68), expressed in outer variables and expanded for small ε, gives

$$f(\eta) = 1 - A_0(1 - \eta) - \varepsilon A_0 + \ldots \tag{69}$$

and comparison with the outer expansions shows that $\beta_0 = A_0 = 1$.

Equation (65) then becomes

$$w_1''' + w_1'' = 2\,e^{-t}. \tag{70}$$

The solution of (70), subject to the boundary conditions (66) is

$$w_1 = (2t + 2 + A_1)\,e^{-t} + A_1(t - 1) - 2. \tag{71}$$

If $f(t) = 1 - \varepsilon w_0(t) - \varepsilon^2 w_1(t)$ is written in terms of the outer variable and expanded for small ε, then

$$f(\eta) = \eta + \varepsilon(1 - A_1 + A_1\eta) + O(\varepsilon^2), \tag{72}$$

and matching with the outer solution shows that $\beta_1 = A_1 = 1$. Proceeding similarly we find that the equation for $w_2(t)$ is

$$w_2''' + w_2'' = (t + 1)\,e^{-t}. \tag{73}$$

The solution of (73), subject to the boundary conditions (66), is

$$w_2(t) = \left(\frac{7t^2}{2} + 15t + 15 + A_2\right)e^{-t} + A_2 t - 15 - A_2, \tag{74}$$

where A_2 is an arbitrary constant. Now $f(t) = 1 - \varepsilon w_0(t) - \varepsilon^2 w_1(t) - \varepsilon^3 w_2(t)$, and putting $f(t)$ in terms of the outer variable and expanding for small ε yields

$$f(\eta) = \eta + \varepsilon\eta + \varepsilon^2(3 - A_2 + A_2\eta) + O(\varepsilon^3). \tag{75}$$

Comparison with the outer solution gives $A_2 = 3 = \beta_2$. The equation for $w_3(t)$ is

$$w_3''' + w_3'' = (16t^2 + 17t - 1)\,e^{-t} + 3\,e^{-2t}. \tag{76}$$

The solution of equation (76), subject to the boundary conditions (66), is

$$w_3(t) = \left(\frac{16t^3}{3} + \frac{81t^2}{2} + 129t + A_3 + \frac{261}{2}\right)e^{-t} - \\ - \frac{3}{4}e^{-2t} + A_3(t - 1) - \frac{519}{4}, \tag{77}$$

where A_3 is an arbitrary constant. If

$$f(t) = 1 - \sum_{n=0}^{3} \varepsilon^{n+1} w_n(t)$$

is expressed in the outer variable and expanded for small ε, then

$$f(\eta) = \eta + \varepsilon\eta + 3\varepsilon^2\eta + \varepsilon^3(18 - A_3 + A_3\eta) + O(\varepsilon^4) \tag{78}$$

and matching with the outer expansion yields $A_3 = 18 = \beta_3$. The outer expansion has the form

$$f(\eta) = \eta + \varepsilon\eta + 3\varepsilon^2\eta + 18\varepsilon^3\eta + O(\varepsilon^4), \tag{79}$$

and the inner expansion becomes

$$f(t) = 1 - \varepsilon(t - 1 + e^{-t}) - \varepsilon^2[(2t + 3)\,e^{-t} + t - 3] -$$
$$- \varepsilon^3\left[\left(\frac{7t^2}{2} + 15t + 18\right)e^{-t} + 3t - 18\right] -$$
$$- \varepsilon^4\left[\left(\frac{16t^3}{3} + \frac{81t^2}{2} + 129t + \frac{297}{2}\right)e^{-t} - \frac{3}{4}e^{-2t} + 18t - \frac{591}{4}\right] +$$
$$+ O(\varepsilon^5), \tag{80}$$

where $t = (1 - \eta)/\varepsilon$. Equation (80) gives the value of $f''(1)$, which is proportional to the skin friction at the wall,

$$\left(\frac{d^2f}{d\eta^2}\right)_{\eta=1} = -\frac{R}{2} + 1 + \frac{10}{R} + \frac{86}{R^2} + O\left(\frac{1}{R^3}\right). \tag{81}$$

This value is sensitive to changes in the Reynolds number, and is therefore useful as a basis for comparison of numerical and theoretical results.

The solutions (79) and (80) together correspond well with numerical results. Table IV shows values of $f''(1)$ against R for large

TABLE IV

	Section V(ii) $-f''(1)$			Section IV $-f''(1)$	
R	numerical	analytical	R	numerical	analytical
9.871	4.6	2.1	30.978	20.2	14.1
10.610	4.5	2.7	37.952	19.6	17.7
15.275	4.8	5.6	41.993	20.7	19.7
20.040	6.2	8.3	51.954	24.96	24.76
29.582	11.1	13.4	62.241	29.96	29.94
35.482	14.8	16.4	72.439	35.06	35.07
39.574	17.3	18.5	92.480	45.11	45.12
51.475	24.2	24.5	99.038	48.40	48.41
59.006	28.21	28.31	103.05	50.41	50.42
62.159	29.83	29.90	122.81	60.31	60.32
72.426	35.04	35.06			
82.499	40.10	40.12			

Numerical and analytical values of $-f''(1)$ for large suction Reynolds numbers (section IV and V(ii) solutions).

suction Reynolds numbers for both section IV and section V solutions. For values of R greater than approximately 70, the theoretical and the numerical solutions agree to three significant figures for both sections IV and V, which suggests that asymptotically there is no difference between the two branches of the solution for large suction, and that the difference must lie in exponentially small terms, even within the boundary layer.

Equation (79) shows that as $R \to \infty$ the limiting profile $f'(\eta)$ tends to a uniform velocity outside the boundary layer with a sharp discontinuity at the wall as the axial velocity falls to zero. This is typical of both section IV and section V profiles and suggests again that the perturbation solution is valid for both branches of the large suction solution.

In order to distinguish between the two solutions obtained numerically the outer expansion will now be examined in more detail.

7.3. *Modified outer expansion.* The outer expansion $f = \sum_0^\infty \beta_n \varepsilon^n \eta$ was obtained from (55) by considering only terms of order ε^n, and the solution was such that no information was found about $f''(\eta)$ and higher derivatives, which are exponentially small. An examination of numerical results suggests that the difference between the two solutions for large suction is in the exponentially small terms, which were neglected in the matching process, so the outer expansion will now be modified to include these terms to find a possible reason for duality.

It will be assumed that, in (55)

$$\beta = \sum_{n=0}^{\infty} \beta_n \varepsilon^n + \alpha_1(\varepsilon) = \alpha_0 + \alpha_1 \tag{82}$$

where $O(\alpha_1(\varepsilon)) < \varepsilon^n$ for all n. A perturbation of the outer solution of the form

$$f(\eta) = \alpha_0 \eta + g(\eta) \tag{83}$$

is considered. Substitution of β and $f(\eta)$ from (82) and (83) into (55) yields

$$\varepsilon(\eta g''' + g'') + 2\alpha_0 g' - \alpha_0 \eta g'' = 2\alpha_0 \alpha_1. \tag{84}$$

The boundary conditions at the centre of the pipe become

$$g(0) = 0, \quad \lim_{\eta \to 0} \eta^{\frac{1}{2}} g''(\eta) = 0. \tag{85}$$

The solution of (84) subject to the boundary conditions (85) is

$$g(\eta) = \alpha_1\eta + \gamma_0\eta\left(1 - \alpha\eta + \frac{\alpha^2\eta^2}{6}\right), \tag{86}$$

where $\alpha = \alpha_0/\varepsilon$, and where α_1 and γ_0 are arbitrary constants. For (86) to be a valid approximation, $\gamma_0\alpha^2$ must be exponentially small. Then

$$f(\eta) = (\alpha_0 + \alpha_1)\,\eta + \gamma_0\eta\left(1 - \alpha\eta + \frac{\alpha^2\eta^2}{6}\right). \tag{87}$$

This solution will now be compared with the solutions obtained numerically to see if any guide can be obtained concerning the differences between the two numerical solutions.

From (87), $f''(\eta^*) = 0$ when $\eta^* = 2/\alpha = 2\varepsilon(1 + \varepsilon + 3\varepsilon^2 + \ldots)^{-1}$. This implies that a turning point of $f'(\eta)$ exists at this point. Since $f'''(\eta) = \alpha^2\gamma_0$, then $f'(\eta^*)$ is a minimum for $\gamma_0 > 0$, and is a maximum for $\gamma_0 < 0$. This is confirmed by numerical results, where section IV solutions have a minimum at approximately $\eta^* = 2\varepsilon$, and section V(ii) solutions have a maximum value at this point.

Further justification for the solution (87) is found by considering the ratio

$$\frac{f'''(0)}{f''(0)} = -\left(\frac{1}{2\varepsilon} + \frac{1}{2} + \frac{3\varepsilon}{2} + \ldots\right).$$

This ratio again agrees with numerical results for both section IV and section V(i) solutions.

As a further check on the validity of the solution given by (87), the constant γ_0 was evaluated for R equal to 72.43 and 72.44, the cases in which the solutions had been obtained for sections V(ii) and IV, respectively.

From equation (87)

$$\gamma_0 = -f''(0)\,\varepsilon/2\alpha_0$$

and, using the values of $f''(0)$ given by the numerical solutions it is found that $\gamma_0 = \pm 5.9 \times 10^{-7}$. With this value of γ_0 the solution (87) accurately predicts the numerical solutions for both section IV and section V(ii) in the range $0 \leqslant \eta \leqslant 0.6$.

No further progress could be made to find a method of evaluating

γ_0. Since the difference between the two solutions appears to lie in this constant, it would be of interest to know whether such a method can be found.

Received 16 January 1968
In final form 17 February 1969

REFERENCES

[1] BERMAN, A. S., J. Appl. Phys. **24** (1953) 1232.
[2] TERRILL, R. M., Aero. Quart. **XV** (1964) 297.
[3] TERRILL, R. M., Aero Quart. **XVI** (1965) 323.
[4] BERMAN, A. S., Effects of porous boundaries on the flow of fluids in systems with various geometries, paper No. p/720 Proc. Sec. Intern. Conf. on Peaceful Uses of Atomic Energy (United Nations), Geneva (Switzerland) 1958.
[5] WHITE, F. M., J. Appl. Mech. **29** (1962) 203.
[6] YUAN, S. W. and A. B. FINKELSTEIN, Trans. ASME **78** (1955) 719.
[7] MORDUCHOW, M., Quart. J. Appl. Math. **XIV** (1957) 361.
[8] WEISSBERG, H. L., Phys. Fluids. **2** (1959) 510.
[9] ECKERT, E. R. G., P. L. DONOUGHE, and B. J. MOORE, Velocity and friction characteristics of laminar viscous boundary layer and channel flow over surfaces with ejection or suction, NACA Report TN 4102, NACA, Washington (D.C.) 1957.